

Chemical and Electrochemical Studies of *para*-Hydroazopyrazolone Derivatives as Corrosion Inhibitors for Mild Steel in Hydrochloric Acid Solutions

A.S.Fouda^{1*}, S.M. Abd El-Wahab², M.S.Attia², A.O.Youssef², H.O. Elmoher^{2,3}

¹Chemistry Department, Faculty of Science, Mansoura University, Mansoura-35516, Egypt,

²Chemistry Department, Faculty of Science, Ain Shams University, Cairo, Egypt.

³Quality Control Section Head, South Dabaa Petroleum Company (Dapetco).

*E-mail: asfouda@hotmail.com

Received: 24 April 2015 / Accepted: 11 July 2015 / Published: 12 August 2015

A comprehensive study on the inhibitory effect of some *para*-Hydroazopyrazolone (antipyrine) derivatives verse mild steel corrosion in 1 M HCl solution has been performed by chemical method(WL), electrochemical techniques (Tafel polarization, electrochemical frequency modulation (EFM) and electrochemical impedance spectroscopy (EIS)) at 25°C. The efficiency of inhibition rose with addition of inhibitor and decreased with raising temperature. Data of Tafel polarization reveals that these investigated compounds reduced both the anodic and cathodic reactions and thus behaved as mixed-type inhibitors. The ability of these molecules to adsorb on the surface of mild steel best fit with Langmuir's adsorption isotherm. The thermodynamic activation parameters of mild steel corrosion in 1 M HCl were determined and discussed. Scanning electron microscopy and energy dispersive X-ray (SEM & EDX) techniques were employed for surface examination of uninhibited and inhibited mild steel. A good correlation was found between the experimental results and the theoretical data. The % inhibition efficiency (%IE) results from different experiments were in a reasonable agreement.

Keywords: Corrosion inhibition, mild steel, *para*-Hydroazopyrazolone, HCl, SEM, EDX

1. INTRODUCTION

Our studies are aimed to revealing the mode of interaction of some *para*- Hydroazopyrazolone (antipyrine) derivatives with the metal surface, extent of formation of metallic chelates and measure the corrosion rate for mild steel in aqueous solutions . In addition to study the stability of organic derivatives in acidic media and spectrophotometric determination of dissolved iron in the corrosive media. On the other hand, compare the corrosion inhibition data obtained from weight loss with that

obtained from Tafel extrapolation, EIS and EFM techniques. Also the morphology of mild steel surface by scanning electron microscopy and energy dispersed X-ray (SEM & EDX) reported before and after exposing it to the aggressive medium. This work reveals a correlation between the theoretical data and the experimental results hoping to get some general ideas to guide the composing of inhibitor in reality.

Mild steel has been extensively used under different conditions in petroleum sector [1]. Also, it is utilized under different conditions in allied and chemical industries. Aqueous solutions of HCl used in acid pickling, acidification of petroleum wells and the removing of scales are more efficient, economical and straight forward with respect to other acids reagents [2]. The most problem face mild steel uses is its low corrosion resistance in acidic environment. Many methods used recently to reduce this problem. The use of inhibitors is one of these minimizing methods. Generally, organic molecules with O, N, and S atoms are employed as inhibitors to retire the corrosion of mild steel in HCl medium [3-4]. Several researchers investigated the use of heterocyclic compounds on dissolution of steel in acid environment [5-11]. Organic molecules containing N atom are effectively used as corrosion inhibitors in HCl medium, while compounds containing sulfur are sometimes used for H₂SO₄ medium [12]. It was proven that oxygen ligands generally form stable and strong ferric chelates, while nitrogen ligands form more stable ferrous chelates [13-14].

It is generally assumed that “the adsorption of the inhibitor at the metal/solution interface is the first step in the mechanism of inhibition in aggressive media”. Amar et al. [15] reported that “Four types of adsorption may occur by organic compounds at the metal/solution interface: (1) electrostatic attraction between the charged metal and the charged molecules, (2) interaction of uncharged electrons pairs in the molecule with the metal, (3) interaction of π -electrons with the metal and (4) combination of (1) and (3)”. Physisorption is regarded to electrostatic attractive forces between the electrically charged metal surface and inhibiting molecules ions or dipoles. Chemisorption includes the transfer or share of charge from inhibitor molecules to the surface to establish a coordinate bond. For transition metals having vacant low energy electron orbital, electron transfer is preferred. Also, for inhibitors compounds having relatively loosely bound electron, electron transfer can be expected [16]. A reduction of either the cathodic or the anodic reaction or both arises from the adsorption of inhibitor on the corresponding active sites [17-18]. Fouda et al. [19] stated that” The percent of inhibition efficiency (%IE) is obviously dependent on the strength of adsorption and this, in term, is affected by the number of adsorption sites and their charge density, molecular size, heat of hydrogenation, mode of interaction with the metal surface and extent of formation of metallic complexes”.

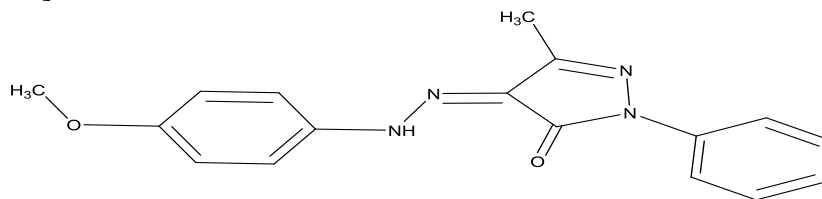
2. EXPERIMENTAL METHODS

2.1. Chemical additives and solutions

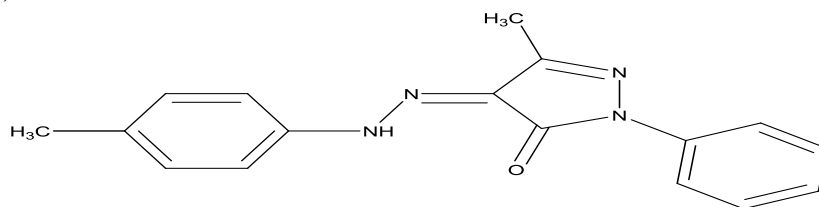
a) *Hydrochloric acid* (37 %), absolute ethanol, sodium chloride, sodium carbonate and propanone were purchased from Al-Gomhoria Company, Egypt

b) Antipyrine derivatives as inhibitors

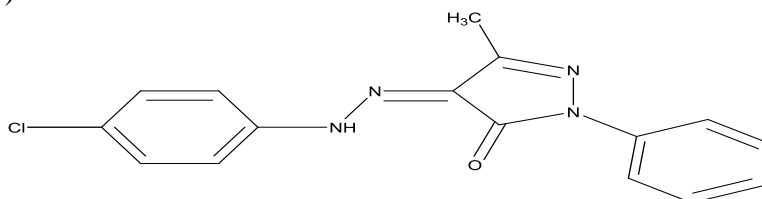
Para-Hydroazopyrazolone derivatives (Antipyrine) ligands (A, B & C) were synthesized as described before [20, 21]. These additives are shown below:



(A) (Z)-4-(2-(4-methoxyphenyl)hydrazono)-5-methyl-2-phenyl-2,4-dihydro-3H-pyrazol-3-one
Chemical Formula: $C_{17}H_{16}N_4O_2$
Molecular Weight: 308.34



(B) (Z)-5-methyl-2-phenyl-4-(2-(p-tolyl)hydrazono)-2,4-dihydro-3H-pyrazol-3-one
Chemical Formula: $C_{17}H_{16}N_4O$
Molecular Weight: 292.34



(C) (Z)-4-(2-(4-chlorophenyl)hydrazono)-5-methyl-2-phenyl-2,4-dihydro-3H-pyrazol-3-one
Chemical Formula: $C_{16}H_{13}ClN_4O$
Molecular Weight: 312.76

(C)

(c) Hydrochloric acid Solution

A stock solution of 6M HCl was prepared from concentrated chemically pure grade acid and titrated against standard solution of sodium carbonate to check the concentration of the prepared acid. For our study, 1M HCl was prepared by diluting the stock solution with bidistilled water.

(d) Sodium chloride solution

The aggressive solutions for studying pitting corrosion were made of freely aerated 3.5% NaCl, which has a comparable salt level to that of seawater. A stock solution of sodium chloride (2M) was prepared. Clear solution of 3.5% NaCl, was repeated by diluting a volume of a stock solution with bidistilled.

(e) Inhibitors solutions

100 ml stock solutions (10^{-3} M) of para-Hydroazopyrazolone derivatives were prepared by dissolving a defined weight of each derivative in a specific volume of ethyl alcohol, then the solution completed up to the 100 mark with bidistilled water.

2.2. Materials

Chemical composition of mild steel (weight %) which used in this study is: 0.13 C, 0.04 P, 0.6 Mn, 0.05 S and the balance is Fe.

2.3 Methods Used for Corrosion Measurements

2.4.1. Weight loss measurements

Rectangular coupons of mild steel “with dimensions 1 x 1 x 2 cm” were polished with different grades of emery paper sizes (400, 800, 1200 and 2000), afterward degreased with propanone, washed with bidistilled water and dried carefully. Coupons were immediately immersed in 1 M HCl with or without various concentrations of the investigated organic derivatives. The efficiency of inhibition (% IE) and surface coverage degree of metal (θ) have been calculated using following equation:

$$\% \text{ IE} = \theta \times 100 = [1 - (\Delta W_{\text{inh}}/\Delta W_{\text{free}})] \times 100 \quad (1)$$

Where, ΔW_{free} and ΔW_{inh} are the weight losses of mild steel per unit area in uninhibited and inhibited solutions at a given period of time and temperature, respectively.

2.4.2. Electrochemical measurements

Electrochemical techniques, namely electrochemical frequency modulation (EFM) potentiodynamic polarization and electrochemical impedance spectroscopy (EIS) were utilized in our study. A typical three-compartment glass cell was used in these experiments. It is consisted of saturated calomel electrode (SCE) as a reference electrode, a platinum foil (1 cm^2) as a counter electrode and mild steel specimen as working electrode (1 cm^2). The reference electrode was connected to a Luggin capillary and the tip of the Luggin capillary is made very close to the surface of the working electrode to minimize IR drop. The cell was open to air and the measurement was performed at room temperature under unstirred conditions. All potential values were recorded against SCE. Before every experiment, the electrode polished with successive different grades of emery paper, then degreased with propanone. After that, the coupons were washed gently with bidistilled water. Then, the working electrode was immersed in the solutions and the open circuit potential was recorded when it became virtually constant.

All the electrochemical studies were performed using Gamry Instrument Series G750™ Potentiostat / Galvanostat / ZRA with Gamry applications include DC105 software for potentiodynamic measurements, EFM140 software for EFM measurements, and EIS300 software for EIS measurements. Echem Analyst 5.5 Software installed in a laptop computer was used for graphing, plotting and fitting data.

a- Potentiodynamic polarization measurements

Curves of potentiodynamic polarization were resulted by changing potential of the electrode automatically from -1200 to +200 mV with regard to open circuit potential at a scan rate of 1 mV s⁻¹. Stern-Geary method [22] can be used for the computation of corrosion current density. The extrapolation of cathodic and anodic Tafel lines of charge transfer controlled corrosion reactions to a point which yields log i_{corr} and the corresponding corrosion potential (E_{corr}) for blank solution and for each concentration of inhibitor. Afterward, i_{corr} was employed for calculation of (% IE) inhibition efficiency and (θ) surface coverage as the following:

$$\% \text{ IE} = \theta \times 100 = [1 - (i_{\text{corr (inh)}} / i_{\text{corr (free)}})] \times 100 \quad (2)$$

Where, $i_{\text{corr (free)}}$ and $i_{\text{corr (inh)}}$ are the corrosion current densities with and without the investigated organic derivatives, respectively.

b- Electrochemical impedance spectroscopy (EIS) measurements

EIS experiments were performed using Ac signals at a definite corrosion potential in a frequency range of 100 mHz to 100 kHz with amplitude of 5 mV peak to peak. The efficiency of inhibition (%IE) of the inhibitor has been found out from the charge transfer resistance values using the following Eq. [23]:

$$\% \text{ IE}_{\text{EIS}} = \theta \times 100 = [1 - (R_{\text{ct}} / R_{\text{ct}}^{\circ})] \times 100 \quad (3)$$

Where, R_{ct}° and R_{ct} are the charge transfer resistance in the absence and of presence of the investigated derivatives, respectively. The interfacial double layer capacitance (C_{dl}) values were obtained [24] by using the following equation:

$$C_{\text{dl}} = Y_0 (\omega_{\text{max}})^{n-1} \quad (4)$$

Where, Y_0 = CPE coefficient, (ω_{max}) = the frequency at which the imaginary part of impedance ($-Z_i$) has a maximum and (n) is the CPE exponent (phase shift).

c- Electrochemical frequency modulation (EFM) measurements

Electrochemical frequency modulation (EFM) employed as a nondestructive and rapid technique for corrosion rate measurements without previous knowledge of Tafel constants. The larger peaks were utilized to figure out the corrosion current density (I_{corr}), the Tafel slopes (β_c and β_a) and the causality factors CF2& CF3 [25-26]. The steady state of the coupons was attended after 30 min. % IE_{EFM} calculated as in Eq. (2)

2.4.3. Surface morphology

The surface of mild steel coupons was prepared by immersed coupons in 1 M HCl for 72 hours with and without the ideal concentrations of investigated derivatives, after polished with successive different grades of emery paper, and then degreased with propanone. After that, the coupons were washed gently with bidistilled water, dried carefully and hanged into the spectrometer without any further treatment. Scanning electron microscopy and energy dispersive X-ray (SEM & EDX) techniques model JEOL JXA-840A electron probe micro analyzer were employed for surface examination of uninhibited and inhibited mild steel coupons.

2.4.4 Spectroscopic Analysis

Hach DR 3800 spectrometer, 10 cm stoppered silica cells, normal scan speed ,bandwidth of 2.0 nm, in the spectral range 320-900 nm at $25 \pm 1^\circ\text{C}$ use for the following:

i- Studying the stability of the inhibitors in acidic medium

The electronic spectra of the inhibitor solution (21×10^{-6} M) in the presence and absence of 1M HCl and after immersion of the mild steel specimen for 6 hours at $25 \pm 1^\circ\text{C}$ were measured [27].

ii- The spectra profile of inhibitors

The spectra of the inhibitors solution were recorded as well as the formed film on the surface of mild steel that dissolved by a definite volume of pure ethyl alcohol.

iii- Determination of total dissolved iron

Coupons were immersed in acid solutions with and without addition of inhibitor concentration (21×10^{-6} M) at 25°C for 6 hours. The amount of iron dissolved in the solution for both uninhibited and inhibited samples was determined by spectrophotometry at $\lambda_{\text{max}} = 510$ nm using 1, 10 Phenanthroline [28] or FerroVer Iron Reagent [29].

2.4.5. Quantum chemical calculations

Materials Studio DMol3 [30-31] version 4.4.0, Accelrys Inc. San Diego, CA, program was used for performing all the quantum chemical calculations. The following quantum chemical indices were considered; HOMO energy (the highest occupied molecular orbital), LUMO energy (the lowest unoccupied molecular orbital), dipole moment (μ), energy gap, ΔE ($\Delta E = E_{\text{LUMO}} - E_{\text{HOMO}}$) of the investigated organic derivatives.

3. RESULTS AND DISCUSSION

3.1. Weight loss measurements

Figure (1) exhibits the weight loss–time curves for the dissolution of mild steel in 1 M HCl with and without different ratios of compound (A). Curves for other derivatives (B & C) acquired and are not demonstrated. Results of Table (1) illustrated that, the efficiency of inhibition increments with increment in the inhibitor concentration from 1×10^{-6} to 21×10^{-6} M.

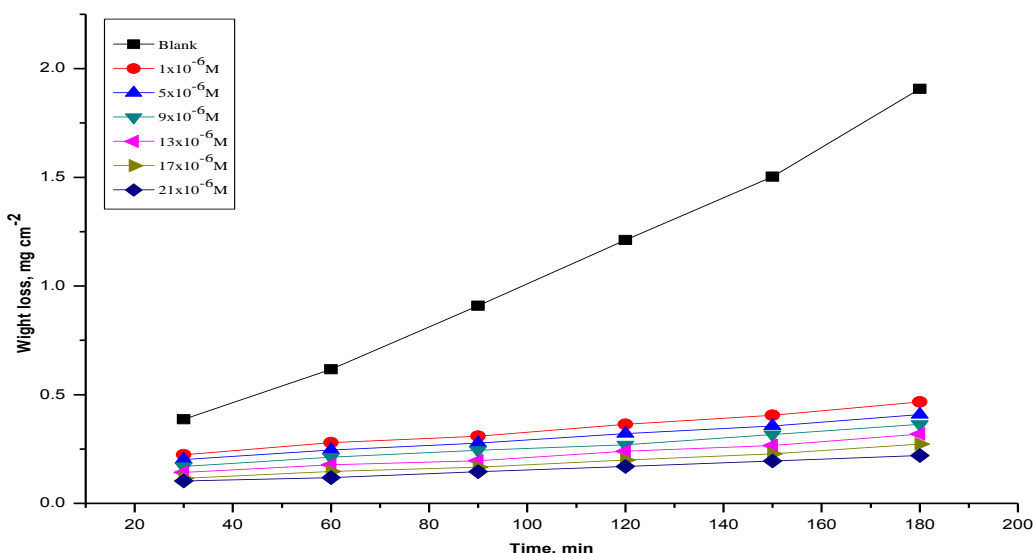


Figure 1. Weight loss-time curves for the dissolution of mild steel in 1 M HCl with and without different ratios of compound (A) at 25°C.

Table 1. Corrosion rate (CR) and the efficiency of inhibition (% IE) for the dissolution of mild steel in 1 M HCl with and without different ratios of investigated organic compounds at 25°C by weight loss method.

Conc., M	Compound (A)		Compound (B)		Compound (C)	
	CR (mg cm ⁻² min ⁻¹) x10 ⁻³	% IE	CR (mg cm ⁻² min ⁻¹) x10 ⁻³	% IE	CR (mg cm ⁻² min ⁻¹) x10 ⁻³	% IE
Blank	10.02	-----	10.02	-----	10.02	-----
1×10^{-6}	2.70	73.0	3.04	69.7	3.34	66.7
5×10^{-6}	2.38	76.3	2.70	73.7	2.94	70.7
9×10^{-6}	2.11	78.9	2.34	77.0	2.54	74.6
13×10^{-6}	1.78	82.3	2.00	80.4	2.23	77.7
17×10^{-6}	1.52	84.8	1.75	83.5	1.95	80.5
21×10^{-6}	1.30	87.0	1.47	86.6	1.61	83.7

The maximum inhibition efficiency was accomplished at 21×10^{-6} M. This pattern can be explained by the isolation of mild steel surface from the solution by the film deposits on its surface [32-34]. The inhibition efficiency (% IE) has a tendency to diminishing in the following sequence: $A > B > C$.

3.1.2. Adsorption isotherms

Deriving the adsorption isotherm that describes the metal/inhibitor/ environment system is one of the most adequate methods of implying adsorption quantitatively [35]. At different concentrations of the investigated derivatives, values of (θ) the degree of surface coverage were estimated in 1 M HCl solution. Trials were done to fit (θ) values to distinguish adsorption isotherms. Langmuir’s adsorption isotherm was fitted well with the experimental results. Draw of (C/θ) vs (C) for all concentrations of investigated derivatives are illustrated in Figure (2). Straight lines relationship for the studied compounds was acquired. The relation between (ΔG°_{ads}) standard adsorption free energy (K_{ads}) equilibrium constant of adsorption as follow [36, 37]:

$$K_{ads} = 1/55.5 \exp(-\Delta G^\circ_{ads}/RT) \tag{5}$$

Table 2. Thermodynamic data for the adsorption of the investigated derivatives in 1 M HCl on mild steel at temperature 25°C.

Inhibitor	$K_{ads} \times 10^{-4} M^{-1}$	Slope	R^2	$-\Delta G^\circ_{ads} kJ mol^{-1}$
A	133.19	1.13	0.99734	44.9
B	107.22	1.15	0.99662	44.5
C	100.17	1.17	0.99559	44.2

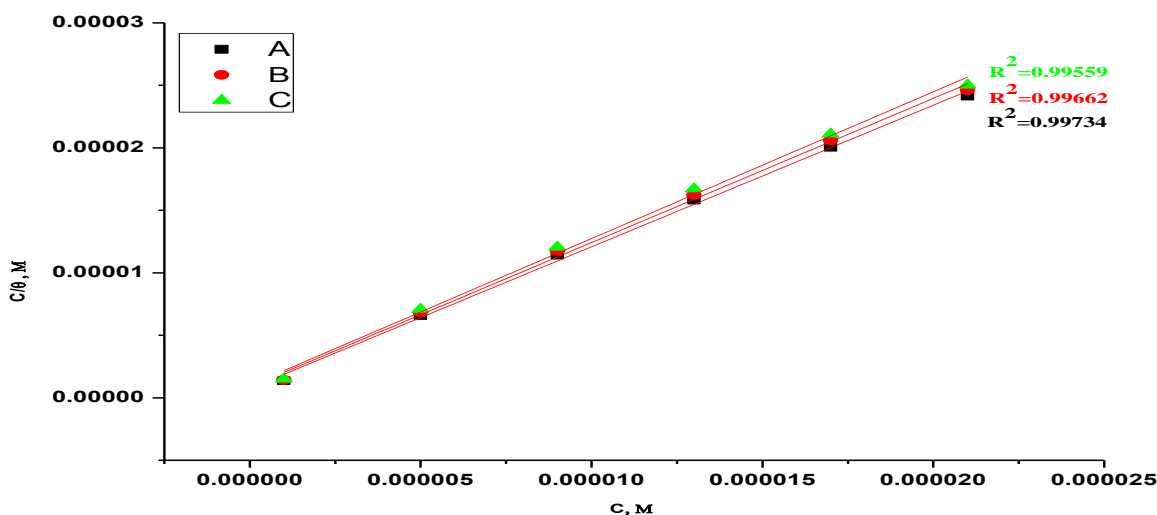


Figure 2. Langmuir adsorption isotherm of the investigated derivatives at 25°C.

The $\Delta G^{\circ}_{\text{ads}}$ and K_{ads} values for investigated derivatives were estimated and are illustrated in Table (4). $\Delta G^{\circ}_{\text{ads}}$ has a negative values indicate that these derivatives are strongly adsorbed with spontaneity process [38] on mild steel surface at all the studied temperature ranges. Due to the desorption of investigated derivatives from mild steel surface, the adsorption diminishes with the increment in temperature.

Values of $\Delta G^{\circ}_{\text{ads}}$ illustrated that the adsorption of these derivatives on surface of the mild steel is not a pure one (i.e. physisorption and chemisorption). Values of K_{ads} confirmed that these derivatives are adsorbed on surface of mild steel in a strong way [39] and hence imply better inhibition [40]. These values are in the same trend to the % IE ($A > B > C$). Laque et al. [41] explained this agreement as “This result reflects the increasing capability, due to structural formation, on the metal surface”.

3.1.3. Effect of temperature

The temperature impact on the corrosion rate and IE% of mild steel with and without different dilution of investigated derivatives was studied by WL measurements in the temperature range of 25 to 55°C. It was observed that, the corrosion rate expanded as the temperature increments and diminishes as the derivatives concentrations increases for all utilized compounds. The activation energy (E_a^*) of the corrosion process was figured as follow:

$$k = A \exp (- E_a^* / R T) \quad (6)$$

Where, k = corrosion rate and A = Arrhenius constant.

Figure (3) gives the Arrhenius plot with and without different ratios of compound A (Curves for other derivatives (B & C) acquired and are not demonstrated here). From Table (5), the value of E_a^* for blank solution is lower than that for inhibited solutions, indicating that the process of mild steel dissolution is slow in the presence of inhibitors and can be attributed to physisorption[42]. It is realized that the values of E_a^* and corrosion rate are contrariwise. This case can be attributed to the development of a film on the mild steel surface working as an energy obstruction for mild steel corrosion [43]. Theory of transition state is utilized for the calculation of Enthalpy (ΔH^*) and entropy (ΔS^*) of activation, as follow:

$$k = [k' / N h] \exp [\Delta S^* / R] \exp [- \Delta H^* / R T] \quad (7)$$

Where, k' = Boltzmann constant, N = Avogadro's number and h = Planck's constant.

Table 5. Parameters of thermodynamic activation with and without various concentrations of the undertaken derivatives.

Inhibitor	Concentration $\times 10^6$ M	E_a^* kJ mol^{-1}	ΔH^* kJ mol^{-1}	$-\Delta S^*$ $\text{J mol}^{-1} \text{K}^{-1}$
blank	1 M HCl	27.6	13.1	143.6
A	1	39.0	18.1	116.1
	5	39.4	18.2	115.9
	9	39.8	18.4	115.7
	13	41.1	19.0	112.7
	17	42.1	19.4	110.7
	21	42.9	19.8	109.3

B	1	37.4	17.4	120.8
	5	37.8	17.5	120.5
	9	38.4	17.8	119.5
	13	39.5	18.3	116.8
	17	40.2	18.6	115.6
	21	41.4	19.1	113.1
C	1	36.1	16.8	124.4
	5	36.9	17.3	122.8
	9	37.8	17.5	120.9
	13	38.3	17.8	120.2
	17	39.1	18.1	118.7
	21	40.6	18.7	115.4

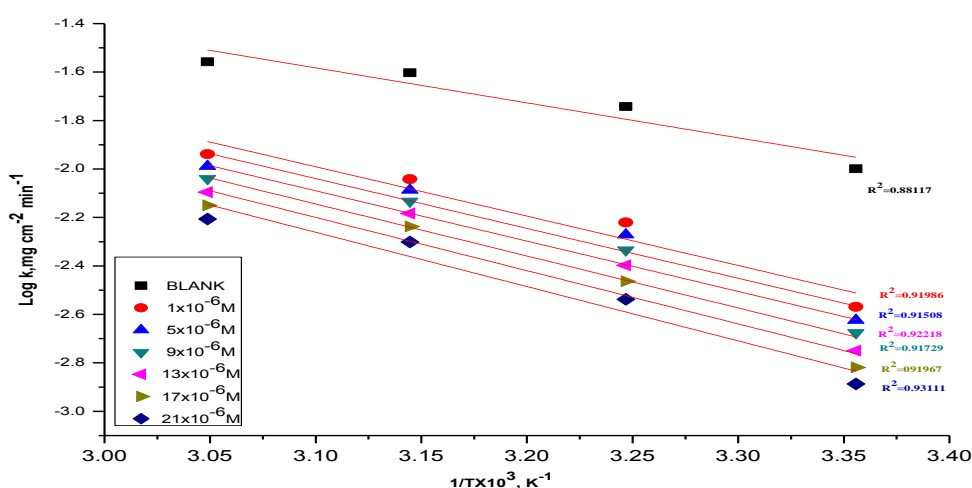


Figure 3. Arrhenius diagram for dissolution of mild steel with and without various concentrations of compound (A).

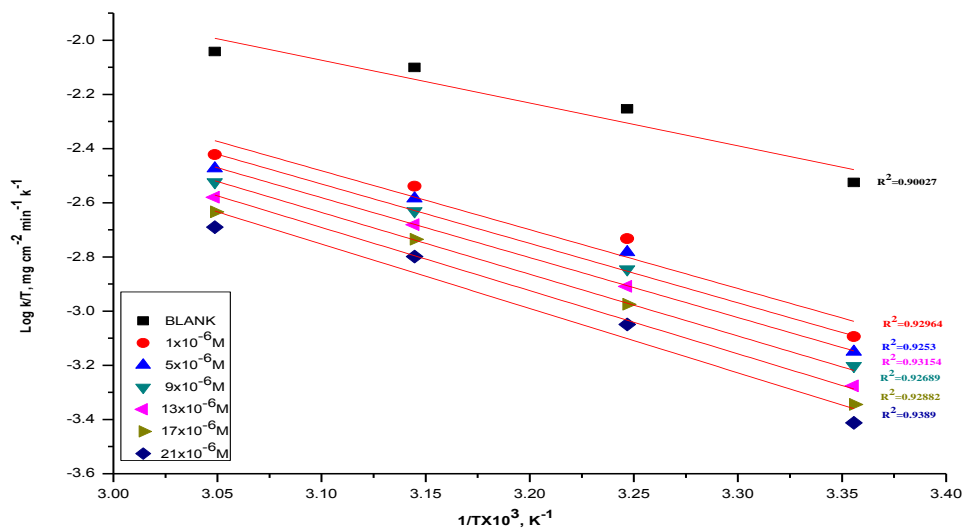


Figure 4. Relation of (log k / T) and (1/ T) for dissolution of mild steel with and without different concentrations of compound (A).

Relation between $\log(k/T)$ and $1/T$ for mild steel with and without different ratios from investigated derivatives give straight lines as given in Figure (4) for compound A (curves for other derivatives (B & C) acquired and are not demonstrated here). ΔH^* has a positive sign which indicate that the dissolution of mild steel is endothermic process. Values of ΔS^* are large and negative reveal that decrease in disordering happened on going from reactants to the activated complex [44]. These values are in the same trend to the % IE ($A > B > C$).

3.2. Electrochemical measurements

3.2.1. Potentiodynamic polarization measurements

Plots of cathodic and anodic Tafel polarization for mild steel with and without various ratios of compound (A) at 25°C are given in Figure (5), (Curves for other derivatives (B & C) acquired and are not demonstrated here).

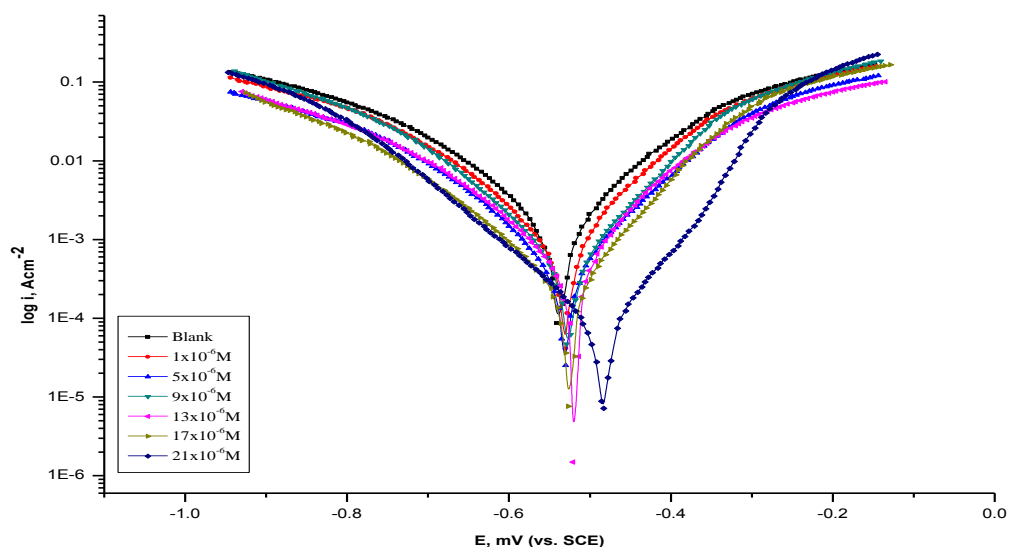


Figure 5. Curves of potentiodynamic polarization for the dissolution of mild steel with and without various concentrations of compound (A) at 25°C.

The studied derivatives affect cathodic hydrogen discharge reactions and the promoting retardation of anodic dissolution of mild steel. Electrochemical parameters such as Tafel constants (β_a and β_c), corrosion potential (E_{corr}), corrosion current density (i_{corr}), inhibition efficiency (%IE) and degree of surface coverage (θ) were figured and are given in Table (6).

Curves are shifted to more positive and more negative potentials with regard to the blank curve by addition of the investigated derivatives. This behavior demonstrated that the studied derivatives behave as cathodic and anodic inhibitors [45, 46]. As the inhibitor concentration increased, the corrosion current density (i_{corr}) decreased but β_a and β_c are approximately constant referred to the

retardation of cathodic and anodic reactions were influenced without changing the dissolution mechanism [47-49].

Table 6. Parameters of potentiodynamic polarization studies of mild steel with and without various concentrations of studied derivatives at 25 °C.

Inh.	Conc. x 10 ⁻⁶ M	- E _{corr.} mV vs SCE	i _{corr.} mA cm ⁻²	β _a mVdec ⁻¹	β _c mVdec ⁻¹	C.R. mmyr ⁻¹	θ	% IE
Blank	1 M HCl	538	2.647	195	218	30.73	-	-
A	1	529	1.816	177	214	21.08	0.314	31.4
	5	531	1.422	237	269	16.51	0.463	46.3
	9	526	1.036	155	181	12.03	0.609	60.9
	13	520	0.728	162	190	8.45	0.725	72.5
	17	527	0.408	138	168	4.74	0.846	84.6
	21	484	0.167	117	175	1.88	0.937	93.7
B	1	544	1.925	179	217	22.35	0.273	27.3
	5	541	1.523	174	206	17.68	0.425	42.5
	9	521	1.202	227	251	13.95	0.546	54.6
	13	515	0.813	206	233	9.43	0.693	69.3
	17	525	0.526	143	166	6.10	0.801	80.1
	21	517	0.235	176	203	2.73	0.911	91.1
C	1	532	1.994	178	200	23.14	0.247	24.7
	5	531	1.636	175	199	18.99	0.382	38.2
	9	534	1.276	172	203	14.82	0.518	51.8
	13	514	0.966	229	263	11.21	0.635	63.5
	17	529	0.631	141	172	7.33	0.761	76.1
	21	512	0.303	184	201	3.52	0.886	88.6

3.2.2. Electrochemical impedance spectroscopy (EIS) measurements

Impedance spectra on Nyquist and Bode formats given for the mild steel electrode at definite corrosion potential after 30 min exposure in inhibited and uninhibited solutions of compound (A) is shown in Figure (6). (Curves for other derivatives (B & C) acquired and are not demonstrated here). To varying EIS data, the electrical equivalent circuit (Randles model) given in Figure (7) is used. The circuit comprises of the charge transfer resistance (R_{ct}), capacitance of the double layer (C_{dl}) and the solution resistance (R_s) which fit well with experimental data. Figure (6-A) demonstrated a single semi-circle represented the single charge transfer process during dissolution with regardless the existence of inhibitor molecules.

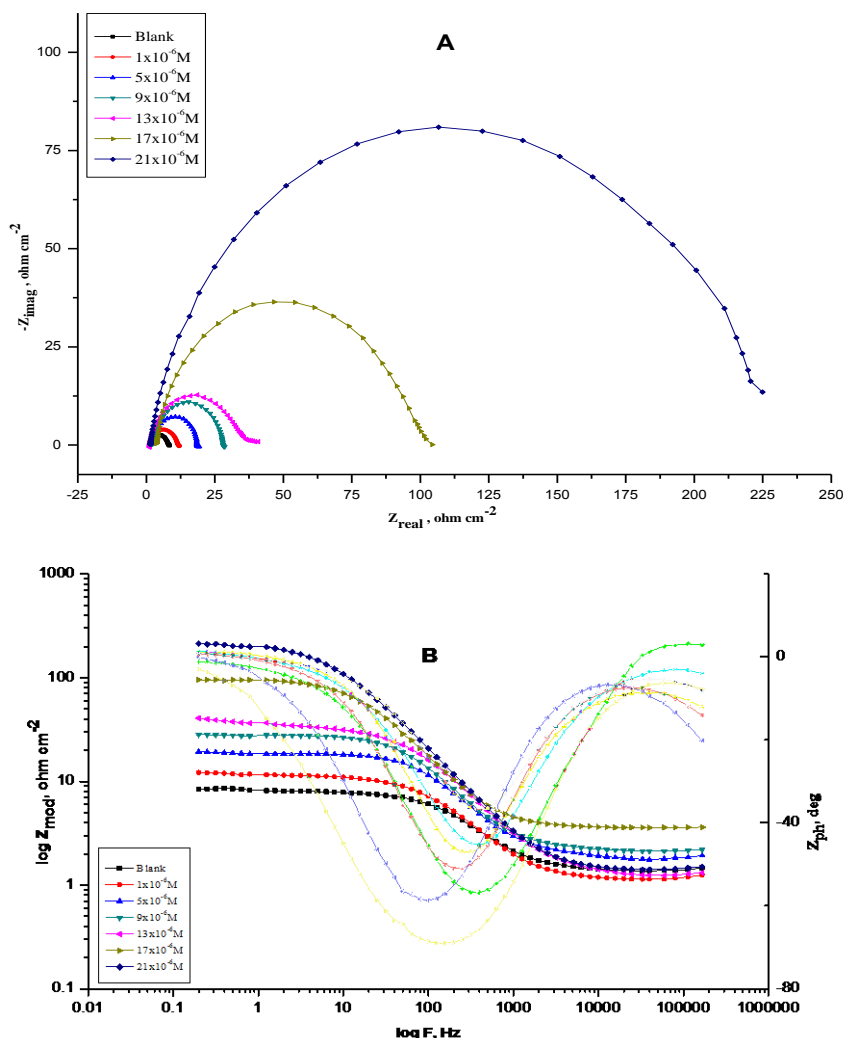


Figure 6 . EIS spectra on Nyquist (A) and Bode (B) format for corrosion of mild steel with and without addition of compound (A) at 25°C.

Variation from ideal circular shape is attributed to the distribution frequency of interfacial impedance which regarded to impurities, adsorption of inhibitors, grain boundaries and inhomogeneity of the electrode surface [50, 51]. Reviews of impedance spectra on the Bode format in Figure (6-B) illustrated that each spectra comprises of a large capacitive loop with one capacitive time constant.

Parameters of EIS measurements are given in Table (7). As the inhibitor concentration increased, R_{ct} values raised and the values of C_{dl} are contrariwise. This can be related to the progressive substitution of water molecules on the metal surface by the inhibitor molecules, reduced the extent of dissolution reaction. As the values of R_{ct} get higher, the metal dissolution get slower [52, 53].The decrease in C_{dl} is attributed to the lower of the local dielectric constant and/or the increase of the electrical double layer thickness proposed that the inhibitor molecules act by adsorption at the mild steel /solution interface. The adsorption can take place either by interaction of the inhibitors with effectively adsorbed chloride ions or between the π -electrons and/or unshared electron pairs of inhibitor molecule and the empty d-orbitals of the metal surface atoms (donor - acceptor interaction)

[54-56]. EIS data demonstrated %IE values with similar pattern to Tafel polarization studies. The variation of %IE values from the two methods may be credited to the distinctive surface status of the electrode in the experiments procedures and/ or the various models that were used for the interpretation [57, 58].

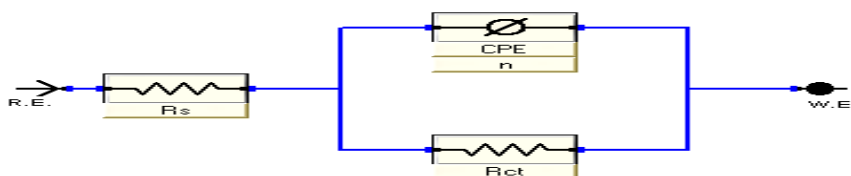


Figure 7. Randles model used to fit EIS data for mild steel/1M HCl interface.

Table 7. EIS data of mild steel for inhibited and uninhibited solutions of undertaken derivatives at 25°C

Comp.	Conc., x106 M	Cdl, μFcm^{-2}	Rct, Ωcm^2	θ	%IE
Blank	1 M HCl	171.10	6.821	---	---
A	1	167.80	10.35	0.341	34.1
	5	116.36	17.09	0.601	60.1
	9	116.37	25.95	0.737	73.7
	13	95.27	38.39	0.822	82.2
	17	120.85	88.82	0.923	92.3
	21	111.58	196.6	0.965	96.5
B	1	145.84	9.263	0.264	26.4
	5	189.86	16.99	0.599	59.9
	9	82.95	25.01	0.727	72.7
	13	100.43	34.92	0.805	80.5
	17	187.91	54.42	0.875	87.5
	21	91.81	93.83	0.927	92.7
C	1	197.76	8.87	0.231	23.1
	5	208.88	12.72	0.464	46.4
	9	81.73	18.07	0.623	62.3
	13	125.45	32.66	0.791	79.1
	17	85.92	46.36	0.853	85.3
	21	109.99	58.99	0.884	88.4

3.2.3. Electrochemical frequency modulation (EFM) measurements

Theory of EFM technique has been previously explained [59, 60]. Figure (8) represented the EFM intermodulation spectrum which consists of the current response as a function of frequency.

Parameters of the electrochemical kinetic are figured out at different concentrations of the investigated derivatives in 1 M HCl at 25°C were listed in Table (8). The inhibition efficiency, % IE

increases by increasing the studied inhibitor concentrations and in a good agreement with other techniques. According to EFM theory, the values of CF-2 and CF-3 (causality factors) are close to 2 and 3 respectively [61-63] which ensure the quality of the measured parameters. The order of the IE% obtained is: $A > B > C$.

3.3. Surface Examination Using SEM–EDX Techniques

Figure (9) illustrates the micrographic of mild steel surfaces obtained with and without the presence of 21×10^{-6} M of the investigated derivatives after exposing for 72 hours. The surface of the blank sample suffers from serious corrosion attack, but the surfaces in the presence of the investigated derivatives, were smoother than the blank one. Due to the development of a film on mild steel surface hence the surface become isolated from the corrosive medium and sequentially denoted excellent inhibition action [64, 65].

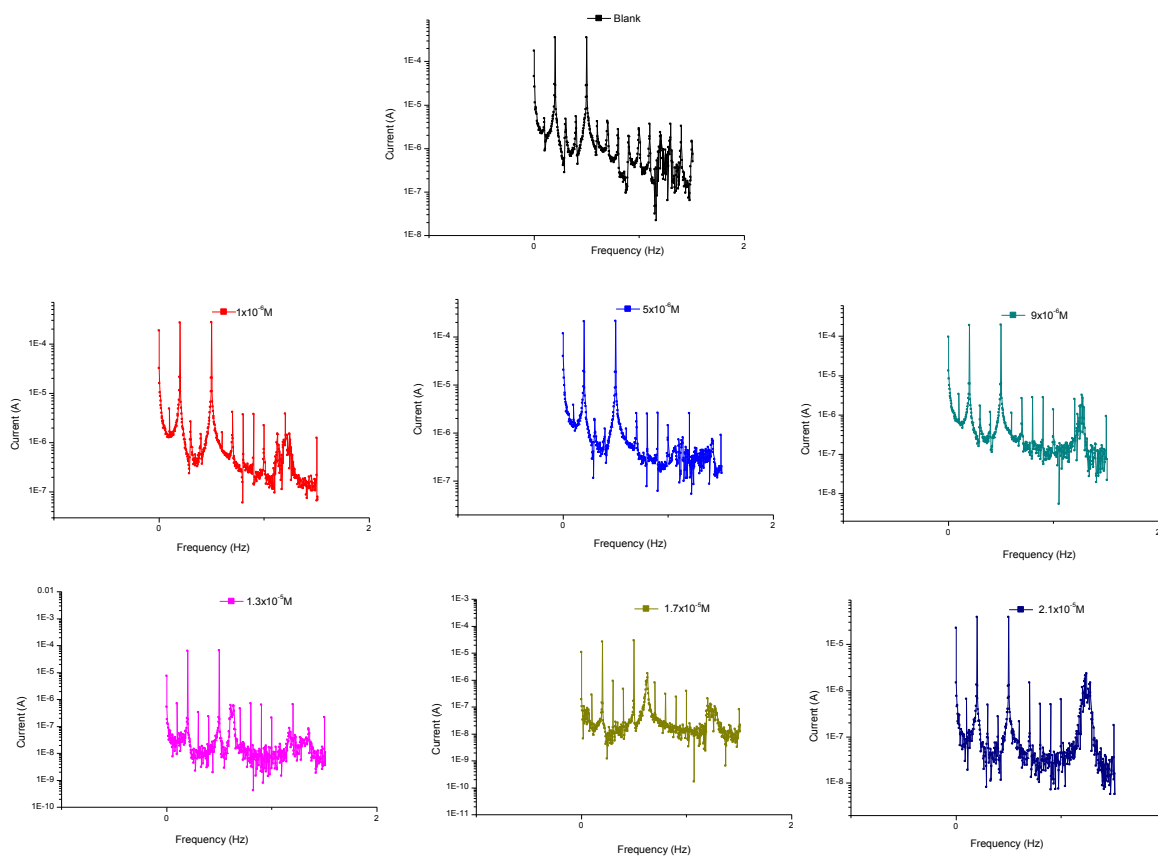


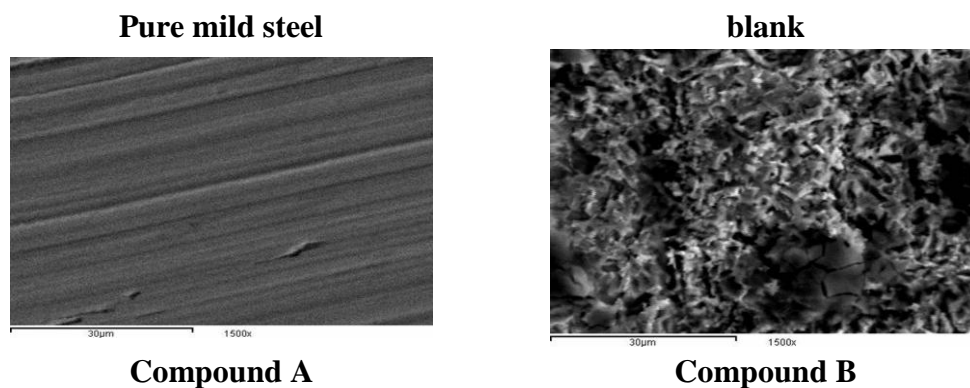
Figure 8. EFM spectra for mild steel with and without various concentrations of compound (A) at 25°C .

Table 8. Parameters of electrochemical kinetic demonstrated by EFM technique for mild steel in 1 M HCl with and without various concentrations of undertaken derivatives at 25°C.

Inh.	Conc. x10 ⁶ M	i _{corr} μAcm ⁻²	β _a mVdec ⁻¹	β _c mVdec ⁻¹	CF-2	CF-3	C.R. mpy	θ	% IE
Blank	1 M HCl	746.4	133	143	1.60	3.09	341.1	-	-
A	1	399.5	92	99	1.85	2.86	182.6	0.465	46.5
	5	317.7	95	102	1.94	2.72	145.2	0.574	57.4
	9	278.1	92	98	1.70	2.82	127.1	0.627	62.7
	13	227.4	21	28	1.58	2.27	103.9	0.695	69.5
	17	132.5	89	181	1.97	3.81	65.4	0.822	82.2
	21	58.0	88	112	1.94	2.78	26.7	0.922	92.2
B	1	476.9	93	99	1.42	2.96	217.9	0.361	36.1
	5	393.2	101	117	2.02	3.04	175.4	0.473	47.3
	9	327.1	104	113	1.72	2.74	149.4	0.562	56.2
	13	257.3	87	94	1.74	2.92	117.6	0.655	65.5
	17	170.1	103	167	2.02	3.59	83.9	0.772	77.2
	21	83.9	99	111	2.01	2.74	37.5	0.888	88.8
C	1	600.0	103	105	1.78	3.08	296.2	0.196	19.6
	5	499.8	65	73	1.95	1.05	246.6	0.330	33.0
	9	373.5	100	105	1.47	3.28	170.6	0.500	50.0
	13	303.0	113	122	1.71	2.71	138.5	0.594	59.4
	17	215.0	89	104	2.04	2.09	106.5	0.712	71.2
	21	94.0	98	122	2.07	2.86	41.9	0.874	87.4

3.3.2. Energy dispersion spectroscopy (EDX) studies

Figure (10) represents the EDX results of mild steel with and without 21x10⁻⁶ M of undertaken derivative. The EDX spectra declared the presence of carbon, nitrogen and oxygen atoms covered the coupon surface which attributed to the inhibitor. This may be confirmed by the absence of nitrogen signal for blank sample as shown in Table (9).



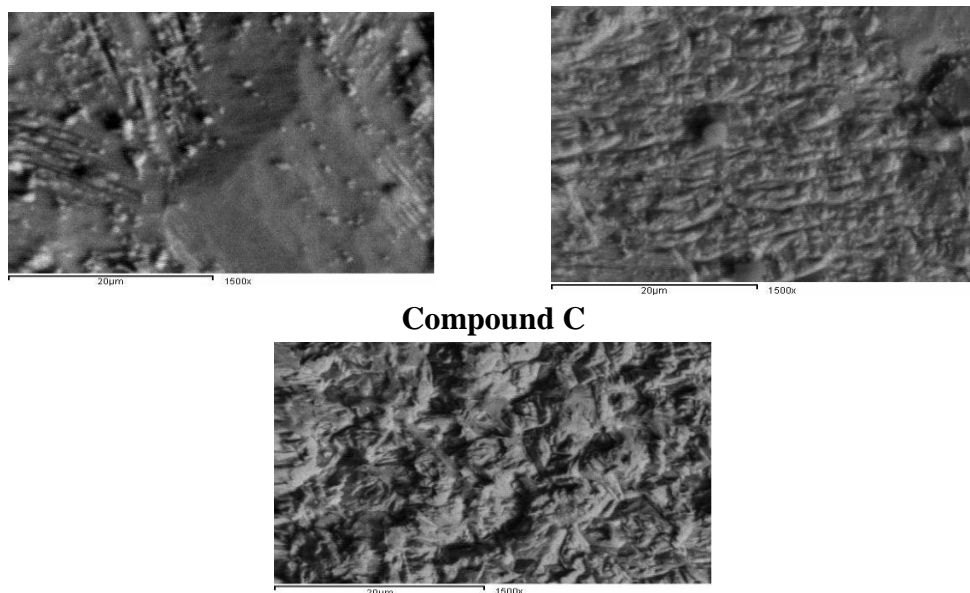
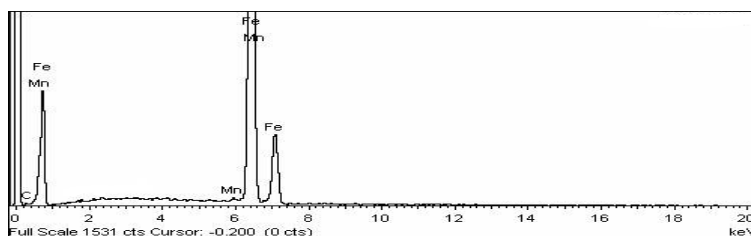


Figure 9. SEM micrographs for mild steel in 1 M HCl with and without the existence of 21×10^{-6} M of investigated derivatives after immersion for 72 hours.

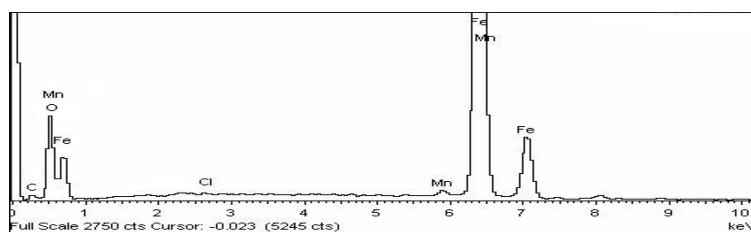
Table 9. Surface composition (weight %) of mild steel in 1 M HCl with and without the existence of 21×10^{-6} M of investigated derivatives after 72 hours of immersion.

(Mass %)	Fe	Mn	C	O	N	Cl
Pure	96.88	0.69	2.43	--	--	--
Blank	59.49	0.66	2.39	37.46	0	0
A	63.82	0.14	18.01	10.63	7.29	0.11
B	62.75	0.11	17.37	12.51	7.14	0.12
C	61.12	0.09	15.81	13.44	7.11	2.43

pure mild steel



Blank



Compound A

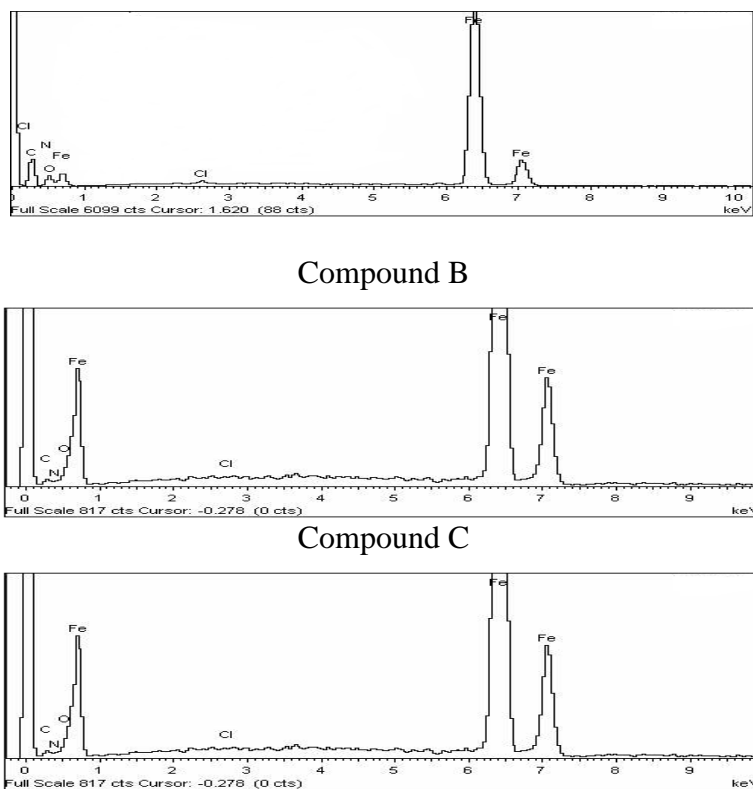


Figure 10. EDX analysis of mild steel in 1 M HCl with and without the existence of 21×10^{-6} M of investigated derivatives after immersion for 72 hours.

3.4. Spectroscopic Analysis

The electronic spectra of investigated derivatives with and without 1M HCl and after immersion of mild steel for different times at 25°C. Figure 11 A-C shows more or less the same bands, which indicates that these derivatives are stable in the acidic medium, but there are noticeable changes in the absorbance value of each band after mild steel exposure in the inhibited solution. This can be explained by the inhibitor concentration reduced in the solution due to the formation of insoluble complex between these inhibitors and the dissolved iron in the acidic medium that deposited on coupon surface [66].

The key legend of Figure 11 as following: (1) Free investigated derivatives (of 21×10^{-6} M), (2) 1M HCl solution containing investigated derivatives (21×10^{-6} M) after 1hour, (3) 1M HCl solution containing investigated derivatives (21×10^{-6} M) after 6 hours, (4) 1M HCl solution containing investigated derivatives (21×10^{-6} M) after immersion of mild steel for 6 hours,(5) Film formed after 3 hours and (6) Film formed after 6 hours.

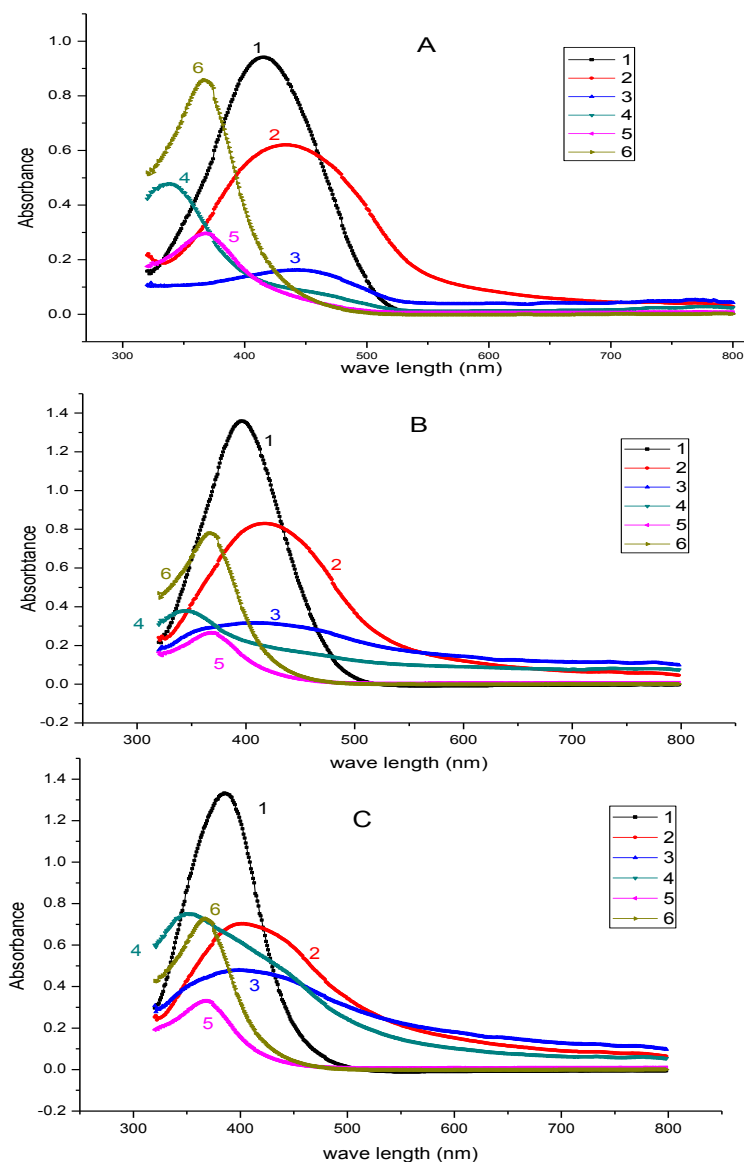


Figure 11. Electronic spectra of the investigated derivatives.

The amounts of dissolved iron measured by the spectrometric method in 1M HCl acid with and without 21×10^{-6} M of investigated derivatives (A–C) after exposing the mild steel coupons for 6 h at 25°C are summarized in Table 10. As shown from this table, the amount of dissolved iron is low in the case of derivatives with respect to blank (1M HCl). This can be mainly attributed to the stable complex film that inhibits metal dissolution by forming a hindrance layer between the metal and the environment, preventing the bare metal contacting the solution i.e., (the dissolution of metal in the existence of studied derivatives is low with respect to the blank). From the amount of dissolved iron, the surface coverage (Θ) and %IE were calculated as follows [67]:

$$\Theta = 1 - A/B \tag{8}$$

$$\%IE = (1 - A/B) \times 100 \quad (9)$$

Where, A is iron content in the existence of inhibitor and B is iron content in blank solution. The calculated values of % IE and θ of the inhibitor towards the dissolution of iron are represented in Table 10. The values of %IE was found to have the following trend $A > B > C$, similar to previously demonstrated results of the studied techniques.

Table 10. Iron content,(ppm) for mild steel in 1M HCl with and without 21×10^{-6} M of investigated derivatives after 6 hours of exposure at 25°C.

Compound	Iron content, (ppm)	(θ)	%IE
Blank	9.98	---	-----
A	2.21	0.7786	77.86
B	2.66	0.7335	73.35
C	3.02	0.6974	69.74

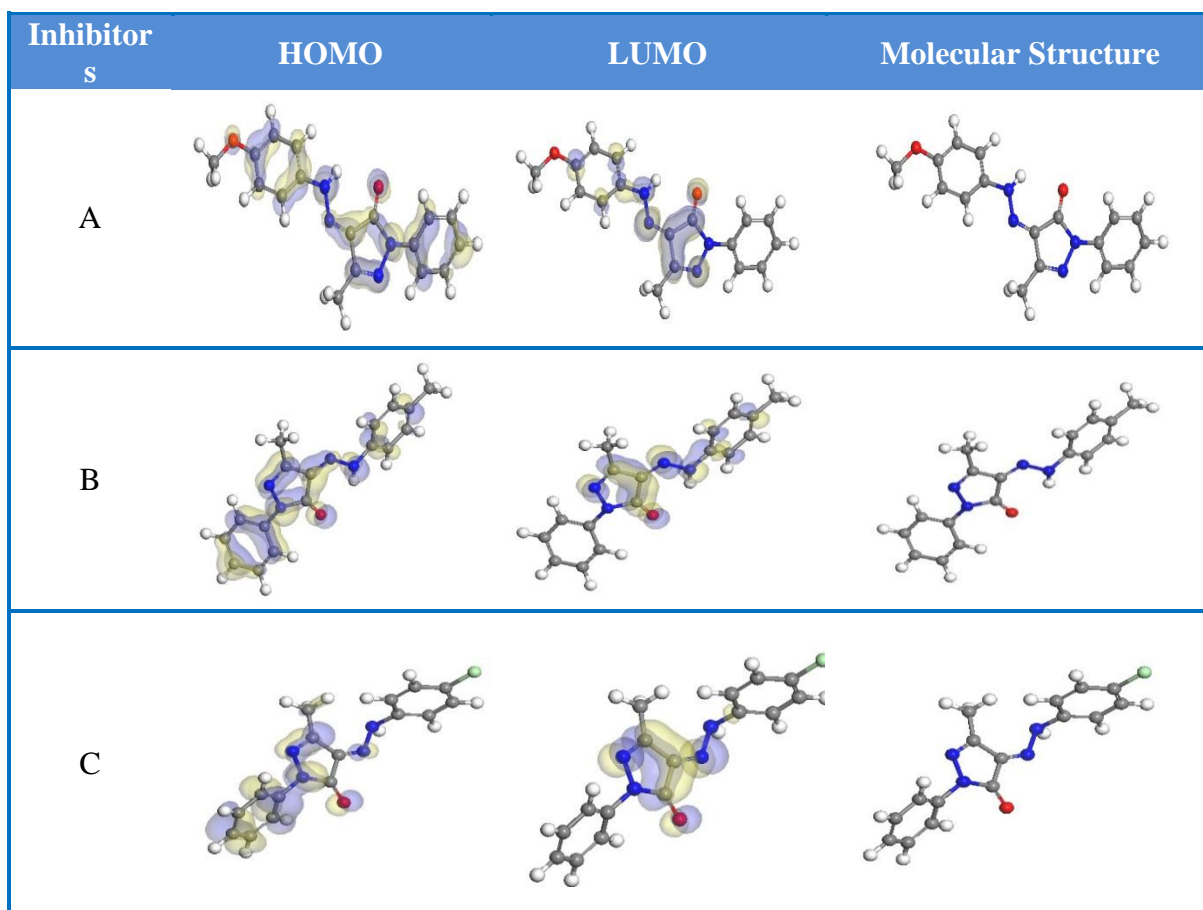
The electronic spectra of free derivative A, corrosive media contain 21×10^{-6} M of derivative A and the removed film are shown in Figure 11 A, as an example. The spectra of shows a band at 415 nm, which is attributed to ($\pi - \pi^*$) and ($n - \pi^*$) transitions, while the spectra of the removed film and spectra of solution show three bands, at 340, 450, and 600 nm, due to intra-ligand, L → M charge transfer, and d-d forbidden transitions of Fe^{3+} ion, respectively [68]. The $n - \pi^*$ transitions undergoes a blue shift indicating that the lone pair electrons of oxygen and nitrogen are coordinated to the metal ion. The lower inhibition efficiency of these derivatives may be related to the lower surface coverage of the surface due to the formation of a complex between these derivatives and Fe^{+2} dissolved in solution, which decreases the concentration of the inhibitor in the solution. Thus, less surface coverage and hence lower inhibition occur [67]. On the other hand, the formed metal inhibitor complex is insoluble in water and, hence, has a large surface area [69] which leads to its precipitation on the metal surface and, therefore, increases the surface coverage and inhibition.

3.5. Quantum chemical parameters of investigated derivatives

Values of quantum chemical indices such as (E_{HOMO} and E_{LUMO}), μ and energy gap ΔE , are calculated. E_{HOMO} and E_{LUMO} responsible for the reactive ability of the inhibitor [70]. Higher E_{HOMO} of the adsorbent leads to higher electron donating ability [71] and hence %IE is increased. The lower, the values of E_{LUMO} , the more favor that the molecule would receive electrons [72]. The calculated quantum chemical indices (E_{HOMO} , E_{LUMO} , μ) of undertaken derivatives are demonstrated in Table 11. The energy band gap ($\Delta E = E_{LUMO} - E_{HOMO}$), which is the energy to kick out an electron from the last occupied orbital, will affect on %IE, and low absolute values of the energy band gap will give higher inhibition efficiencies [73]. The inhibition efficiency decreased in this order: compound (A) > compound (B) > compound (C). Figure12 represented HOMO and LUMO electronic density distributions of these derivatives.

Table 11. Calculated quantum chemical indices for undertaken derivatives

Parameter	A	B	C
-EHOMO (eV)	8.686	8.746	9.221
-ELUMO (eV)	1.107	1.108	1.235
ΔE (eV)	7.579	7.638	7.987
I (eV)	8.686	8.746	9.221
A (eV)	1.107	1.108	1.235
μ (debyes)	3.675	3.575	2.255
Molecular surface area (Å^2)	341.013	332.243	324.369

**Figure 12.** HOMO and LUMO electronic density distributions of the investigated derivatives.

According to Koopmans's theorem [74] the electron affinity (A) and the ionization potential of inhibitor molecules can be calculated as follow:

$$I = -E_{\text{HOMO}} \quad (10)$$

$$A = -E_{\text{LUMO}} \quad (11)$$

From Table 11, it is found that the %IE values increase with decrease of inhibitor ionization potential, which means that the inhibitor behave as an electron donor when hindering the active sites [75].

3.6. Mechanism of Corrosion Inhibition:

The inhibition of iron by organic molecules in aqueous solutions, particularly in acidic medium, has also been investigated extensively. The adsorption of organic compounds can be related to the existence of polar atoms of nitrogen, oxygen and aromatic/heterocyclic rings [76]. Therefore, the available reaction centers are p-electrons of aromatic ring and unshared electron pair of heteroatoms. As the inhibitors have empty orbitals, they can accept electrons from d-orbital of metal to form stable complexes [77]. Figure 13 represents the tautomerism of these derivatives.

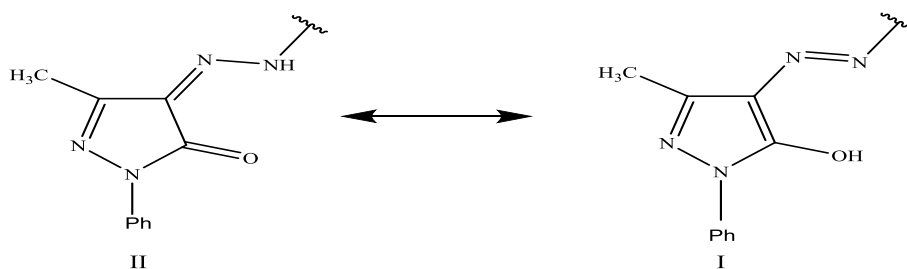


Figure 13. The tautomerism of the investigated derivatives.

The inhibition action of investigated derivative can be illustrated as follows: In the aqueous acidic medium, organic derivatives present either as neutral or protonated



Where, L is organic derivatives. The possible adsorption modes are:

1- The neutral form of (L) may adsorb on the metal surface via the chemisorption mechanism, including the replacement of water molecules from the metal surface and the sharing of electrons between N and O atoms with iron; Figure 14 [20]. The adsorption phenomenon occurs in an aqueous solution containing the organic derivatives [L(aq)]. This includes the replacement of a certain number of water molecules ($n H_2O_{(ads)}$) by the organic derivatives which is adsorbed on the surface [$H_2O_{(ads)}$]. In addition to, the interaction between empty d-orbitals of iron and π -electrons of the aromatic.



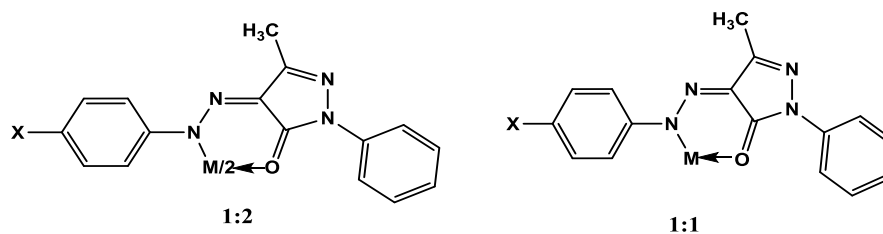
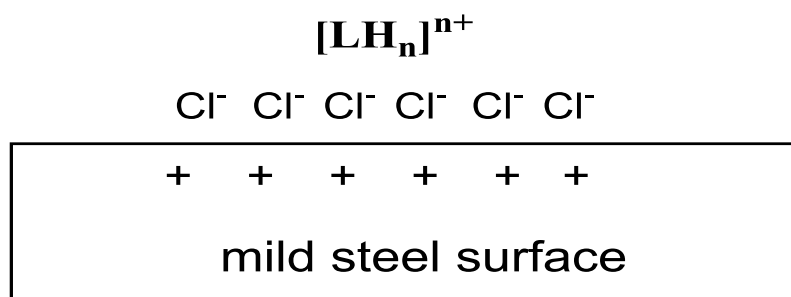
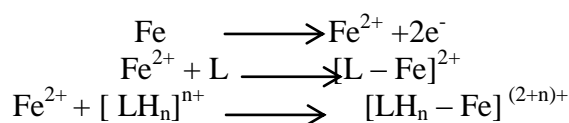


Figure 14. The proposed complex between iron (M) and investigated derivatives (x= p-OCH₃, p-CH₃, and p-Cl)

1. As the mild steel surface charges positive in acid medium [78], electrostatic repulsion take place with the protonated L species. Chloride ions are adsorbed in the surface, which generate an excess negative charge toward the solution and catalysis cations adsorption [79]. Hence the electrostatic interactions can take place with the protonated L and the surface. This means a synergism between L and Cl⁻ that enhances the inhibitive performance of the inhibitor Scheme 1 & 2.

Scheme 1



Scheme 2. Schematic represents of adsorption of investigated derivatives on mild steel surface in 1 M HCl medium.

These chelates might adsorb onto the surface to form a defensive film to isolate the mild steel surface from the aggressive medium [80]. This claim can be supported by spectroscopic results [67]. The film blocks both anodic and cathodic reactive sites on the steel surface. This behavior can be rationalized on the basis of the structure-corrosion inhibition relationship of organic compounds. Linear free energy Relationships (LFER) had been used to correlate the inhibition efficiency of organic compounds with their Hammett constituent constant (σ). The LFER or Hammett relation is given by $\log k (i_{\text{corr.}}) = -\rho\sigma$ as shown in Figure 15 [81, 82] where ρ is reaction constant. Those constituents which attract electrons from the reaction center are assigned positive (σ) values and those which are electron donating have negative σ values. Thus (σ) is a relative measure of the electron density at the reaction center. The slope of the plot of $\log (\text{rate})$ vs. (σ) is (ρ), and its sign indicates whether the

process is inhibited by an increase or decrease of electron density at the reaction center. The magnitude of (ρ) indicates the relative sensitivity of the inhibition process to electronic effects. The large the positive slope of the correlation line ($\rho = +1.85$) shows a strong dependence of the adsorption character of the reaction center on the electron density of the ring, with electron releasing substituents increasing inhibition. Compound A had the highest percentage inhibition efficiency, this is due to present of (p-OCH₃) group which is an electron repelling group with negative Hammett constant ($\sigma_{\text{pOCH}_3} = -0.268$). Compound B comes next in inhibition efficiency because of the existence of (p-CH₃) which is electro donating with a Hammett constant ($\sigma_{\text{pCH}_3} = -0.17$). Compound C comes later, this is due to (p-Cl) group which is electron withdrawing group lead to decreasing the electron density on the molecule with positive Hammett constant ($\sigma_{\text{pCl}} = +0.23$) [83]. Thus, the order of inhibition efficiency of organic derivatives according to three different substituents role, i.e., OCH₃, CH₃, and Cl, is the following: A > B > C.

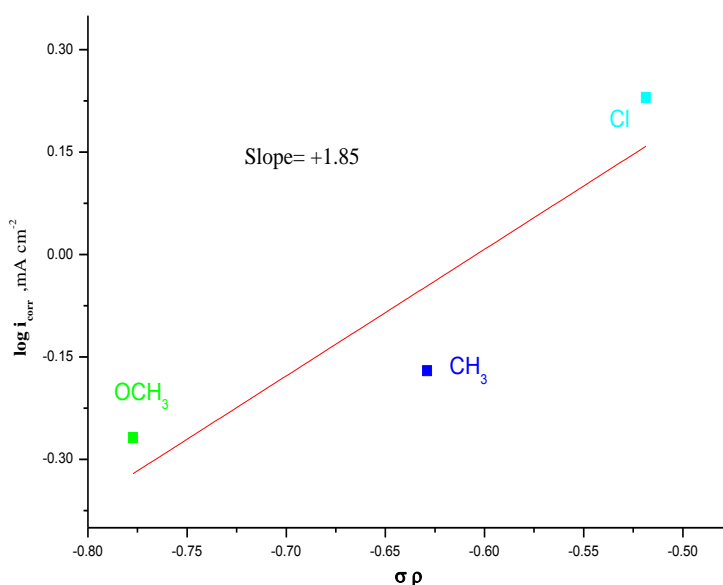


Figure 15. Relation between log corrosion current ($\log i_{\text{corr}}$) and Hammett constant (σ_{ρ}) of the substituents from polarization measurement.

4. CONCLUSIONS

- 1- The investigated derivatives offer inhibiting properties for mild steel in acidic medium.
- 2- The adsorption of these investigated derivatives was found to obey the Langmuir adsorption isotherm.
- 3- Tafel Polarization data shows that the used derivatives behave as mixed-type inhibitor in 1 M HCl.
- 4- The negative value of ($\Delta G_{\text{ads}}^{\circ}$) obtained from this study indicates that these compounds are spontaneously adsorbed on mild steel surface.
- 5- Results obtained from WL, Tafel polarization, EFM, EIS and spectroscopic methods are

reasonably in good agreement.

6- Quantum chemical calculations have been used to study the effect of molecular structure on %IE of the organic compounds.

7- These organic compounds complete the basic requirements to be considered as a corrosion inhibitor.

References

1. A. S. Fouda, A. M. Eldesoky, M. A. Elmorsi, T. A. Fayed and M. F. Atia, *Int. J. Electrochem. Sci.*, 8 (2013) 10219.
2. X. Li, S. Deng, H. Fu, T. Li, *Electrochim. Acta*, 54 (2009) 4089.
3. M. Ajmal, A. S. Mideen, and M. A. Quraishi, *Corros.Sci.* 36 (1994) 79.
4. A. A. Hosary, R. M. Saleh, and A. M. S. Eldin, *Corros. Sci.*, 12 (1972) 897.
5. A. S. Fouda, M. M. Gouda, and, S. I. Abd E-Rahman, *Bull. Korean Chem. Soc.*, 21 (2000)1085.
6. X. Li, S. Deng, H. Fu and G. Mu, *Corros. Sci.*, 51(2009)620.
7. F. Jia-Jun, L. Su-Ning, C. Lin-Hua, W. Ying, Y. Lian-He, and L. De Lu, *J. Mater. Sci.*, 45(2010) 979.
8. S.S. Mahmoud, *J. Mater. Sci.*, 42(2007)989.
9. M. Ozcan, I. Dehri, and M. Erbil, *Appl. Surf. Sci.*, 236(2004) 155.
10. P. Manjula, S. Manonmani, P. Jayaram, and S. Rajendran, *Anti-Corros.Methods Mater*, 48(2001) 319.
11. B.R. Babu and R. Holze, *Br. Corros. J.*, 35(2000) 204.
12. M. Lagren'ee, B. Mernari, M. Bouanis, M. Taisnel and F. Bentiss, *Corros. Sci.*, 44 (2002), 573.
13. N.N. Greenwood and A. Earnshaw, *Chemistry of the Elements*, Pergamon Press, Oxford, England, 1984.
14. H. H. Hamdy, E. Abdelghani , M. A. Amina, *Electrochimica Acta* 52 (2007) 6359.
15. H. Amar, A. Tounsi, A. Makayssi , A. Derja ,J. Benzakour and A. Outzourhit , *Corrosion Science* 49 (2007) 2936.
16. F. Mansfeld, *Corrosion Mechanisms*, Marcel Dekker, New York, (1987).
17. G. Trabaneli, in: F. Mansfeld (Ed.), *Corrosion Mechanism*, Marcel Dekker, New York, (1987).
18. J.G.N. Thomas, *Ann. Univ. Ferrara. N.S., Sez. (Suppl. N.8)* (1981) 453.
19. A. S. Fouda, M. N. Moussa, F. I. Taha and A. I. Elneanaa., *Corros.Sci.* 26 (1986) 719.
20. S. L. Stefan, *MICROCHEMICAL JOURNAL* 35 (1987) 186.
21. H. G. Garg, *the Journal of Organic Chemistry*, 27 (1962)1045.
22. R.G. Parr, D.A. Donnelly, M. Levy and M. Palke. *J.Chem. Phys.* 68 (1978) 3801.
23. F. Bentiss, M. Lagrenee, M. Traisnel and J.C. Hornez, *Corros.Sci.* 41(1999)789.
24. C.H. Hsu and F. Mansfeld, *Corrosion*, 57(2001) 747.
25. R. G. Parr and R.G. Pearson, *J. Am. Chem. Soc.* 105(1983) 7512.
26. R.G. Pearson, *Inorg. Chem.*, 27 (1988) 734.
27. R. M. Silverstein, C. G. Bassler, and T. C. Morrill, *Spectrometric Identification of Organic Compounds*, 3rd ed., John Wiley, New York, (1974).
28. ASTM D 1068 – 05, "Standard Test Methods for Iron in Water." Annual Book of ASTM Standards, Vol 11.01, 2006.
29. Method 8365, *Iron, Total, Powder Pillows*, Edition 5, DOC316.53.01052, HACH COMPANY, 2008.
30. R. Java her dashti, *Anti-Corros, Meth. Mater.* 47 (2000) 30.
31. B. Delley, *J.Chem. Phys.*, 113 (2000) 7756.

32. E. E. Oguzie, C. Unalgbu, C. N. Ogukwe, B. N. Okolue and A. I. Onuchakwu, *Mater. Chem. Phys.*, 84 (2004) 363.
33. A.K. Maayta, and N. A. F. Al-Rawashdeh, *Corros. Sci.* 46 (2004) 1129.
34. J. Aljourani, K. Raeissi, M.A. Golozar, *Corros. Sci.*, 51 (2009)1836.
35. Z.Szklarska-Smialowska; *Electrochemical and Optical Techniques for the Study of Metallic Corrosion*, Kluwer Academic, theNetherlands; 545 (1991).
36. M. Kaminski, and Z. Szklarska-Smialowska, *Corros. Sci.*, 13 (1973) 557.
37. I.K. Putilova, S.A. Balizen, Y.P. Barasanik, *Metallic Corrosion Inhibitors*, Pergamon Press, Oxford (1960).
38. J. D. Talati and D. K. Gandhi, *Corros. Sci.*, 23 (1983) 1315.
39. S. L. F. A. Da Costa and S. M. L. Agostinho, *Corrosion*, 45 (1989) 472.
40. S. S. Abd El-Rehim, S. A. M.Refaey, F. Taha, M. B Saleh and R. A. Ahmed, *J. Appl. Electrochem.*, 31(2001) 429.
41. F. L. Laque and H. R. Gapson; *Corrosion resistance of metals and alloys*; 2nd ed., Reinhold Publishing Corporation, New York, 1963.
42. J. Lipkowski, P.N. Ross (Eds.), *Adsorption of Molecules at Metal Electrodes*, VCH Publishers, New York, (1992).
43. S. L. F. A. Da Costa and S. M. L. Agostinho, *Corrosion*, 45 (1989) 472.
44. E.F. El-Sherbiny, *Mater. Chem. Phys.*, 60 (1999) 286.
45. A.S. Fouda, A.A. Al-Sarawy, E.E. El-Katori, *Desalination*, 201 (2006) 1.
46. H. Amar, A. Tounsi, A. Makayssi, A., Derja, J., Benzakour and A., Outzourhit, *Corros.Sci.* 49, (2007)2936.
47. M.A. Migahed, E.M.S. Azzam, S.M.I. Morsy, *Corros.Sci.* 51(2009)1636.
48. M.N.H., Moussa, A.A., El-Far, A.A., El-Shafei, *Mater.Chem.Phys.* 105(2007)105.
49. M. Benabdellah, R. Touzan, A. Aouniti, A.S. Dafali, S. El-Kadiri, B. Hommouti and M. Benkaddour, *Mater.Chem.Phys.*, 105 (2007)373.
50. E. Bayol, K. Kayakirilmaz, M. Erbil, *Mater.Chem.Phys.* 104 (2007)74.
51. O. Benalli, L. Larabi, M. Traisnel, L. Gengembra, Y. Harek, *Appl. Surf. Sci.*, 253 (2007) 6130.
52. I. Epelboin, M. Keddam, H. Takenouti, *J. Appl. Electrochem.* 2(1972)71.
53. J. Bessone, C. Mayer, K. Tuttner, W. J. lorenz, *Electrochim. Acta*, 28(1983) 171.
54. M. Lebrini, M. Lagrenee, M. Traisnel, L. Gengembre, H. Vezin, F. Bentiss, *Applied Surface Science* 2539 (2007) 267.
55. Gamry Echem Analyst Manual, 2003.
56. K. Babic-Samardzija, C. Lupu, N. Hackerman, A. R. Barron, and A. Luttge, *Langmuir*, 21 (2005) 12187.
57. R.G. Kelly, J.R. Scully, D.W. Shoesmith and R.G. Buchheit, *Electrochemical. Techniques in: Corrosion Science and Engineering*, Marcel Dekker Inc., New York, 2002.
58. R. W. Bosch, W. F. Bogaerts, and B. Syrett, Simple and robust external reference electrodes for high-temperature electrochemical measurements, Proceedings of the 8th International Symposium on Electrochemical Methods in Corrosion Research Modulation (EFM) Technique, Nieuwpoort, Belgium, 4–9 May (2003).
59. R.W. J. Bosch Hubrecht, W.F. Bogaerts, B.C. Syrett, *Corrosion*, 57 (2001) 60.
60. R.W. Bosch and W.F. Bogaerts, *Corrosion*, 52 (1996) 204.
61. E.A. Noor and A.H. Al-Moubaraki, *Mater. Chem. Phys.*, 110 (2008) 145.
62. M.A. Amin, S.S. Abd El-Rehim, E.E.F. El-Sherbini, O.A. Hazzazi, and M.N. Abbas, *Corros. Sci.*, 51 (2009) 658.
63. M.A. Amin, S.S. Abd El Rehim, and H.T.M. Abdel-Fatah, *Corros. Sci.*, 51(2009) 882.
64. R.A. Prabhu, T.V. Venkatesha, A.V. Shanbhag, G.M. Kulkarni, R.G. Kalkhambkar, *Corros.Sci.* 50 (2008) 3356.
65. G. Moretti, G. Quartanone, A. Tassan, A. Zingales, *Wekst. Korros.*, 45 (1994) 641.

66. M. Abdallah, A. S. Fouda, S. A. Shama and E. A. Afifi, *Afr. J. Pure Appl. Chem.*, 2 (2008) 83.
67. M. N. EL-Haddad, A. S. Fouda, and H.A. Mostafa, *Journal of Materials Engineering and Performance*, 22(8) (2013) 2277.
68. E. Mortel, *Coordination Chemistry*, vol. 1, Van Nostrand Reinhold, New York, 1971.
69. G. Saha and N. Kurmaih, *Corrosion*, 42 (1986) 233.
70. C. Lee, W. Yang and R. G. Parr., *Phys. Rev. B*, 37(1988) 785.
71. R. M. Issa, M. K. Awad and F. M. Atlam, *Appl. Surf. Sci.*, 255(2008) 2433.
72. C. Ogretir, B. Mihci and G. Bereket, *J. Mol. Struct.*, 488 (1999)223.
73. A. Y. Musa, A. Mohamad, A. H. Kadhum, M. S. Takriff, and L. T. Tien, *Corros. Sci.*, 53 (2011) 3672.
74. V. S. Sastri, and J. R. Perumareddi, *Corrosion*, 53(1997) 617.
75. J. M. Costa, and J. M. Lluch, *Corros. Sci.*, 24, (1984), 929.
76. S.S. Abd El-Maksoud and H.H. Hassan, *Mater. Corros.*, 58 (2007) 369.
77. S.L. Li, Y.G. Wang, S.H. Chen, R. Yu, S.B. Lei, H.Y. Ma, and D.X. Lin, *Corros. Sci.*, 41(1999)1769.
78. A. K. Singh, and M. A. Quraishi, *Corros. Sci.*, 52(2010)1529.
79. F. Bentiss, M. Traisnel, and M. Lagrenee, *Corros. Sci.*, 42 (2000) 127.
80. X.-H. Li, S.-D., Deng, and H. Fu, *J. Appl. Electrochem.*, 40 (2010)1641.
81. I.N. Putilova and S.A. Barannik, *Metallic Corrosion Inhibitors* pergamon press, London, (1960) 55.
82. R.T. Morrison, and R.N. Boyd, *Universal Book Stal New Delhi (ED.IV):* (1983)1277.
83. M. Abdallah, *Mater. Chem. Phys.*, 82 (2003) 786.